Effects of fuel distribution on thermal environment and fire hazard

Khan, Aatif Ali; Nan, Zhuojun; Zhang, Xiaoning; Usmani, Asif

RESEARCH ARTICLE

WILEY

Effects of fuel distribution on thermal environment and fire hazard

Aatif Ali Khan[1] | Zhuojun Nan[2] | Xiaoning Zhang[3] | Asif Usmani[3]

[1]University of Canterbury, Christchurch, New Zealand

[2]Delft University of Technology, Delft, the Netherlands

[3]The Hong Kong Polytechnic University, Hung Hom, Hong Kong

Correspondence
Zhuojun Nan, Delft University of Technology, Delft, the Netherlands.
Email: z.nan@tudelft.nl

Abstract

Fire accidents in buildings are occurring and claiming thousands of lives each year. Due to various architectural designs, fire hazards would be unique to each building layout. This paper discusses how fire hazard varies with the arrangement of the fuel inside buildings. To comprehensively present the effect of fuel distribution on fire behaviour, results from large-scale experiments, bench-scale experiments, empirical correlations, and numerical studies are provided. In large-scale fire tests, two different cases of wood cribs were tested to demonstrate the effects of porosity on heat generation and fire spread behaviour. Due to the limitations of experimental conditions, the variation in heat release rate attributable to differences in fuel porosity and surface area has been also qualitatively investigated using a cone calorimeter test. To bring the gap between experimental observations and real-word scenarios, a numerical study is also performed. This study further explores the effects of fuel distribution (considering porosity and surface area of fuel throughout the compartment) and ventilation on fire spread beyond the fire compartment. The computational fluid dynamics (CFD) simulations show how the distribution of fuel in different ways can lead fire to spread beyond its origin, as observed in many fire accidents. The paper suggests that designers should consider such critical fire scenarios in performance-based design.

KEYWORDS
building fires, CFD, fuel distribution, performance-based design

1 | INTRODUCTION

Each year nearly half a million building fires are reported in the United States alone.[1] Despite the regular improvement of the codes and standards, such trend is consistent. Over the last three decades, fires have caused the collapse or severe damage of the structure.[2–5] Since the World Trade Centre (WTC) disaster, several studies have been performed to understand the fire behaviour and structural response to the fire in tall buildings. During the investigation of the WTC towers, a "travelling fire" phenomenon was observed, which is presented by many researchers.[6,7] Some crude design models were proposed based on travelling phenomenon observed in experimental studies. Due to the presence of large open spaces in modern buildings, it is necessary to consider such a phenomenon while evaluating the structural resistance to fire. In the last two decades, a few travelling fire models are proposed, that is, Clifton's travelling fire model,[8] travelling fires methodology (TFM),[9,10] and its subsequent refined versions (i.e., improved TFM[11] and TFM with flame extension[12]), and an extended travelling fire methodology framework.[13–15] However, these models have some limitations, such as consideration of uniform

fire load and pre-defined fire trajectory. Fire load plays a vital role in estimating the severity of a fire and evaluating the fire resistance of a structure. The distribution of fuel can significantly affect the structural fire response due to various fire-spread behaviour, including fire spread rates and fire sizes.[16] When estimating fire load for any kind of occupancy, such as office or residential building, a deterministic value is generally suggested in widely adopted codes and standards.[17] In determining the fire risks to the hotel buildings in Hong Kong, Chow et al.[18] carried out a survey considering fire load as the major parameter while ignoring the influence of the fuel distribution pattern or the packing density of the fuel on fire severity. The fire spread and its severity within a compartment depend on various factors such as ventilation, fuel load, fuel distribution, and so on, and these factors can affect the spread of fire (both vertically and horizontally) and overall structural temperature.[19]

Fire load is generally defined in statistical terms.[20] Khan et al.[21] reviewed various methods used to estimate the fire load for an occupancy. Accurately estimating the fire load is crucial for establishing realistic fire scenarios, which ultimately leads to the development of the performance-based design (PBD) approach. It has been found that fire behaviour is also affected by the structural geometry and the distribution of fuel. Standard methods of fire load calculation often ignore the effects of fuel distribution, which can significantly influence fire behaviour and are vital for structural stability in fire accidents. In the Plasco Building fire accident (19 January 2017, Iran),[4,19,22] due to the presence of a high fuel load and the manner in which the fuel was distributed, the fire spread rapidly and reached the top floor within 30 min of ignition. It took fire less than 4 h to bring the whole building to the ground, where more than 32 people lost their lives. It is clear from these fire accidents that not only the fire load but also the fuel distribution and other factors may lead to a unique fire scenario that can lead to a catastrophe. One of the objectives of PBD is to limit fire spread within a compartment,[23] however, such fire accidents clearly show that fire can spread beyond the room of origin, both internally and externally.[23] It is necessary to include the fire scenarios in PBD that account for these factors. The materials and architecture in modern buildings have changed so fundamentally that the assumptions presented in prescriptive approaches are being seriously questioned, particularly in high-rise buildings. The prescriptive approaches such as implementation of standard and parametric fires may produce misleading results. For example, with high fuel loads on each floor and combustible façades (common in modern buildings) around the perimeter of the building, the fire can be considered fuel-controlled (i.e., the fire is concentrated around the openings or burning outside and will continue until the fuel is consumed). In contrast, the standard and parametric fire curves can only represent ventilation-controlled fire scenarios. From the various experimental studies, it was observed that fire in large compartments was generally fuel-controlled, with little or no effect from ventilation.[24–27] Although significant studies have emphasised on the effects of fire load and ventilation on fire behaviour, limited attention has been given to the effects of fuel distribution and building geometry.

In this paper, to investigate the influence of fuel distribution on compartment fire behaviour, a multifaceted research approach has been employed. As porosity allows for greater airflow, enabling more efficient fuel combustion, the large-scale experiments focus on wood cribs with varying porosities (i.e., spacing between the wooden sticks). Complementing this, a qualitative analysis using a cone calorimeter provides insights into the variations in heat release rate (HRR) due to fuel porosity and surface area, thereby addressing experimental limitations. Bridging the gap to real-world fire scenarios, CFD simulations were used to investigate the effects of air gaps between the fuel and surface area on the variation in HRR and fire behaviour. In the numerical study, the effects of fuel load distribution (different spacings between the fuel) on peak compartment temperatures and fire spread behaviour are evaluated by considering different cases of the same fuel loads. The effects of heat generation and fire duration are also studied in this study. Additionally, it analyses and presents fire scenarios that illustrate how fire can spread to upper floors due to the fuel distribution within the compartment.

2 | EXPERIMENTAL INVESTIGATION

2.1 | Large-scale wood-crib experiment

Due to the enormous uncertainties associated with fire, it may behave differently even if one of the environmental parameters is altered. In the current study, two different fuel distribution patterns with varied porosities (i.e., spacing between the wooden sticks) are investigated to demonstrate the burning behaviour of fire using the same volume of fuel load. In the experiment, wood cribs were set up in two configurations, where porosity was changed for both cases, however, the number of wooden sticks remained the same to keep the same fuel load density. The configurations of the wood cribs with distribution patterns and dimensions of cribs and sticks are presented in Figure 1. The tests were carried out in a large tunnel (140 m long tunnel of an 8 m wide and 5 m high with 4.5 m high protected inner section). The fire phenomenon observed in this study can provide a qualitative and quantitative understanding of the fire spread and intensity of the fire for the same fuel load density but with different configurations. Due to the large aspect ratio of the tunnel (similar to a "slice" of a large open-plan compartment[28]) and sufficient ventilation, the fire could be considered "fuel-controlled" during the whole burning period. The "spruce" type wood cribs were used in the experiment where average density of the wood was 430 kg/m^3 with a moisture content of 14 ± 2%. The heat of combustion (ΔH_c) is estimated as 18 MJ/kg for determining the fuel load in terms of the equivalent weight of wood presented in the Society of Fire Protection Engineering (SFPE) Handbook and other literature.[29]

Two cases were presented in this experiment where Case 1 was considered as "low porosity" (sticks were spaced closely) (Figure 1A), and Case 2 as "high porosity" (sticks were spaced at a larger distance) (Figure 1B) wood cribs. As shown in Figure 1, the fuel bed comprised
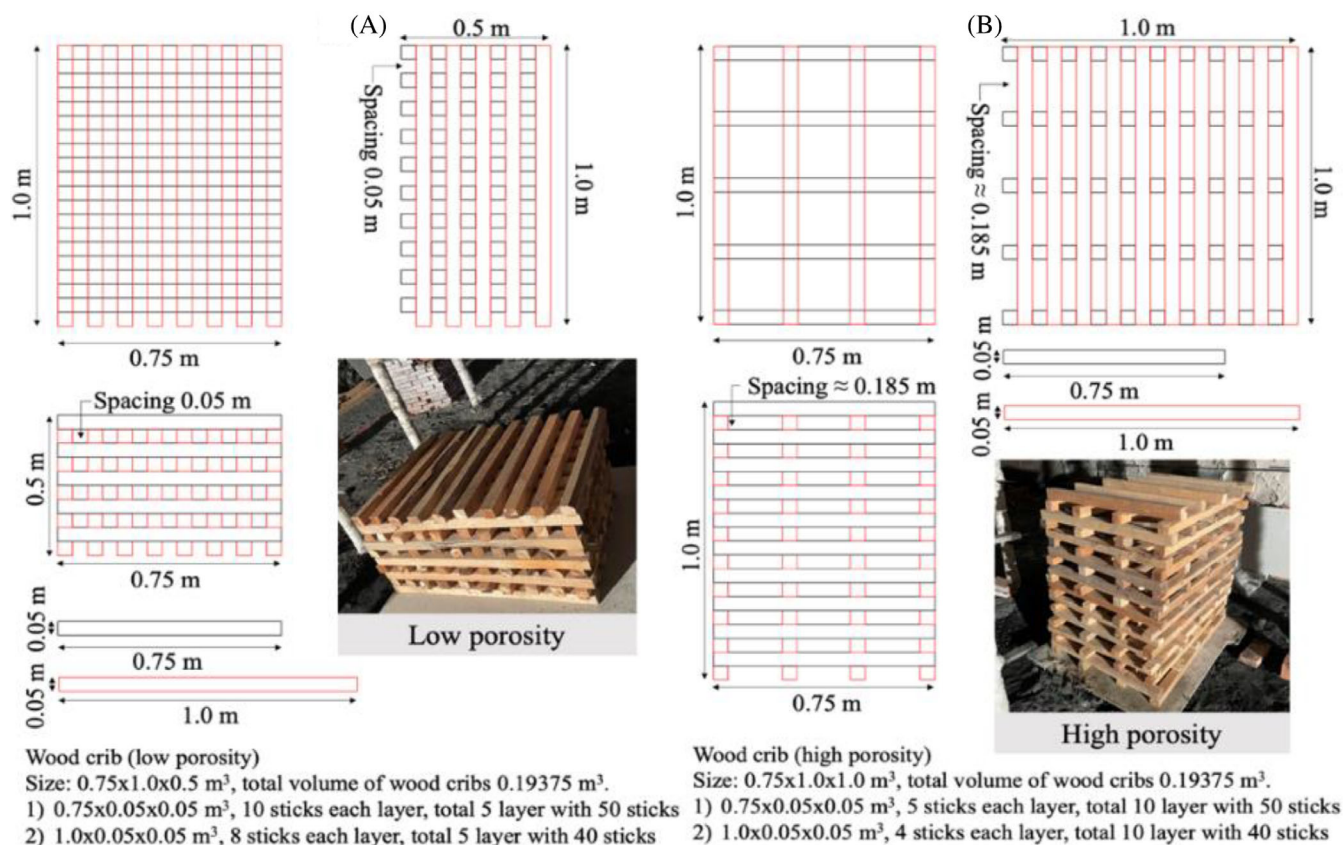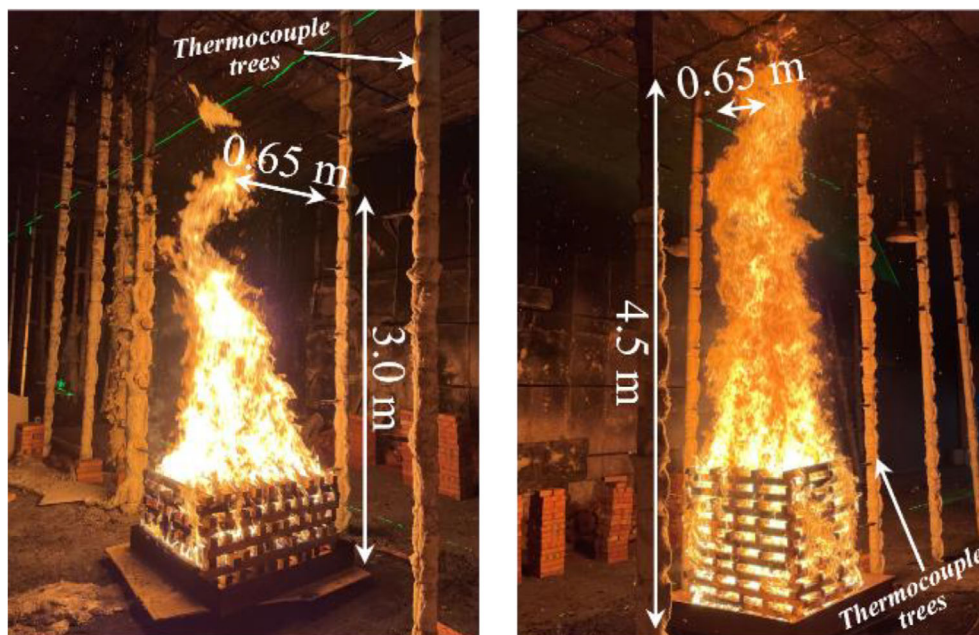
FIGURE 1 The configurations of the wood cribs: (A) Case 1 (low porosity); and (B) Case 2 (high porosity).

FIGURE 2 Maximum flame height for both the configurations of the wood cribs: Case 1 (low porosity) and Case 2 (high porosity).

multiple wooden sticks. For both cases, the same number of sticks was used (50 sticks of $0.75 \times 0.05 \times 0.05$ m^3 and 40 sticks of $1.0 \times 0.05 \times 0.05$ m^3). For Case 1, the spacing between the wooden sticks was 0.05 m, while for the Case 2, the sticks were separated by 0.185 m approximately. The cribs were placed at the centre of the

well-protected test region near an opening of the tunnel. Besides, in the fire laboratory of Sichuan Fire Research Institute (Sichuan, China), several experiments with the same wooden sticks distribution patterns as described above were conducted to investigate fire spread and burning dynamics of non-uniform wood crib.[16]

Temperatures were measured using a set of thermocouple trees equipped with K-type thermocouples, positioned near the fire source. The weighing scales (10 cm high) were placed underneath the fuel bed to measure the mass loss of the wood cribs. Detailed setup information is presented in Appendix A. For both cases, seven wooden sticks soaked in heptane were used as ignitors, and placed at the bottom of the wood crib. Each stick was 0.5 m long with a cross-sectional area of approximately 9 cm^2. The wooden stick ignitors were chosen due to the difficulty in igniting the wooden sticks because of their moisture content. However, these ignitors had an impact on the burning behaviour, for example, accelerating the burning rate and fire spread rate, and increasing the size of fire. The effects of the ignitors should be considered further in future research. Some of the observations are presented in the following sub-sections.

2.1.1 | Fire development and gas temperature

As observed in the tests, the wood stick ignitors impacted the burning behaviour of the wood cribs at the early development stage, approximately 4 minutes until the ignitor's burnout. This included accelerating the evaporation of moisture and the burning rate, as well as increasing the fire spread rate and fire sizes, as shown in Figure 4. After the ignitors burnt out, the burning of the wood cribs reached a stable stage. It is worth mentioning that due to the high porosity of Case 2, there was a noticeable collapse of the wood crib around 12 min after ignition. In comparison, the porosity of Case 1 was lower, resulting in a less significant effect on wood crib collapse. The total fire duration of Case 1 and Case 2 was 19 and 35 min, respectively. Figure 2 shows the maximum flame height reached during the experiment for both cases. In Case 1, the flame reached as high as 3 m during the peak burning rate, while in Case 2, the flame impinged on the ceiling at a height of 4.5 m. It implicates that the flame height can be much larger, and the ceiling would be heated directly by flame for the same fuel load density. It is worth noting that the fuel height was 0.5 m higher in Case 2. According to Hasemi's fire model for localised fire, the flame height depends on the HRR and the diameter of the fire. The HRR of Case 2 is much higher than Case 1[30] (Figure 4).

Figure 3 shows the gas temperatures near the ceilings (around 4.5 m). It is worth noting that the overall temperatures are much lower than expected near the ceiling, it is mainly because of the distance of the thermocouple from the centre of the flaming region, as shown in Figure 2 and Figure A1. The distance from the thermocouple to the centre of the wood crib is 0.65 m. The present experiments demonstrate the localised fire, therefore temperature becomes lower with the radial distance from the centre of the fire.[30] As expected, the gas temperatures for the Case 1 are found to be lower than the Case 2. Other than the lower HRR, another reason for lower gas temperature near the ceiling is the shorter height of the flame. It implies that the structure would be exposed to lower temperatures for a "low porous" fuel load.
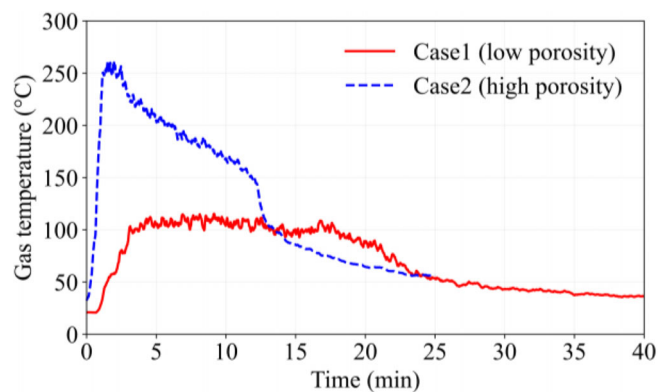

FIGURE 3 Gas temperatures near the ceiling for both the configurations of the wood cribs: Case 1 (low porosity) and Case 2 (high porosity).
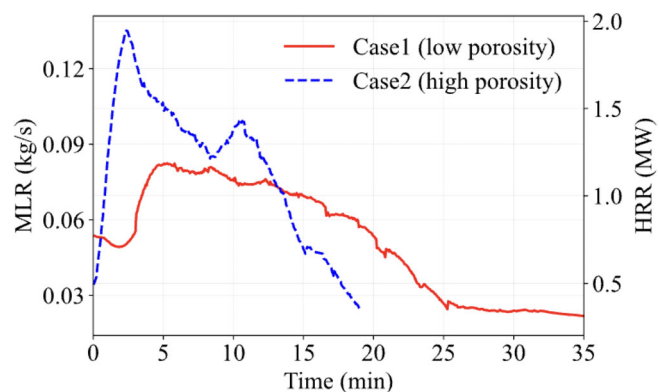

FIGURE 4 The mass loss rate and heat release rate for both the configurations of the wood cribs: Case 1 (low porosity) and Case 2 (high porosity).

2.1.2 | Mass loss rate and heat release rate

Figure 4 shows the mass loss rate (MLR) and HRR for both cases. Since the ignitors are very light, their mass can be neglected. The peak MLR for Case 1 is almost half to Case 2, that is, 0.08 kg/s and 0.14 kg/s for Case 1 and Case 2, respectively. For Case 2, the MLR decreases drastically after 12 min, when the total mass reduces to 20% (Figure 5), while the fuel was burning steadily for Case 1 configuration between 4 and 15 min since the ignition. Due to the high MLR for Case 2, the fuel was burnt out much quicker than Case 1. The fuel was kept burning for 35 min for Case 1, while the fuel was almost consumed fully within 19 min for Case 2. The large duration of the fire (e.g., Case 1) has significant implications on a compartment fire. Although the fuel may burn with lower intensity for low porous fuel distribution, the fire may last longer and keep heating the structure for an extended period. In the 1980s, Law[31] conducted several experiments and proposed an empirical relationship between the mass flow rate and the duration of the fire (Equation 1). As shown in Equation 1, the duration of the fire (τ) is inversely proportional to the mass flow

rate ($\dot{m}_f$) (or burning rate). So, for the same fuel load (L), the case of the lower burning rate would burn for a longer duration, which is Case 1 in these experiments. If the fuel load is high such as in data room, printing room in an office building, the fuel with high porosity may last longer with high intensity (or high heat generation).

$$\tau = \frac{L}{\dot{m}_f} \qquad (1)$$

To estimate the value of the mass flow rate, some empirical correlations for the MLR for wood cribs are presented in SFPE Handbook.[29] The burning rate can be numerically represented as Equation 2. The higher value of porosity contributes to an increase in the burning rate ($\dot{m}$) of fuel as expressed in Equation 2.[29] An experiment conducted by Gross[32] confirmed that the fuel burning rate increased with an increase in fuel porosity. In the current study, Case 1 had lower porosity; therefore, the burning rate was found to be significantly higher for Case 2.

$$\dot{m} = 4.4 \times 10^{-4} \left(\frac{S}{H} \right) \left(\frac{m_o}{D} \right) \qquad (2)$$

where m_o and D are the initial mass and thickness of the fuel, respectively. S is the distance between the stacks (porosity between the fuel), and H is the total height of the fuel load. Although the porosity hugely influences the burning rate, the inverse effect of H was not apparent in the observed behaviour.

MLR is calculated for understanding the HRR for both cases. The rate of fuel burning can be evaluated using Kawagoe's equation,[26] however, it is worth noting that it is generally applicable for ventilation-controlled fires.[21,26] Figure 4 also presents HRR for both cases. To estimate the HRR using MLR, Equation 3 is employed where η represents the combustion efficiency. The value of η is taken as 0.8 from the literature.[33] The peak HRR approached 2 MW for Case 2, while the peak value for Case 1 was around 1 MW. Such fire behaviour may lead the fire to spread much quicker and generate a high-intensity fire. In small compartments, flashover may reach quicker due to high heat fluxes from the flames and the thermal feedback of heated surfaces. In terms of the fire intensity, a 1 MW fire itself may cause severe damage to the structure and the duration of the fire would play a significant role. Figure 5 shows the ratio of the remaining mass with respect to time, that is, the ratio of the remaining mass (m_r) to the original mass (m_o). Almost 70% of the fuel was consumed in the first 10 min for Case 2. On the other hand, it took around 18 min for Case 1.

$$\text{HRR}(t) = \eta Hc \text{MLR}(t) \qquad (3)$$

2.2 | Bench scale calorimeter test

The full-scale experiments (in the previous section) discuss, qualitatively and quantitatively, the effect of porosity, however, the surface area was the same for both the fuel configurations. The rate of heat
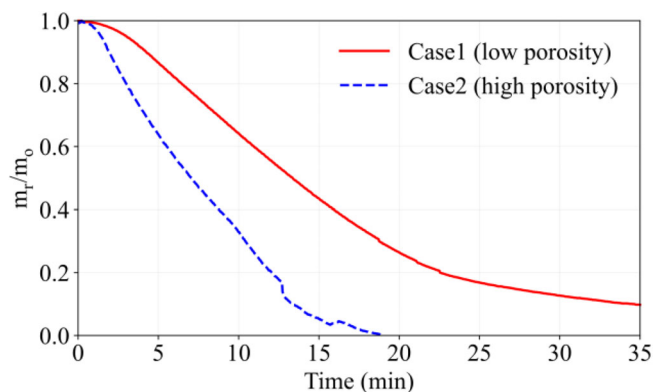

FIGURE 5 The ratio of the remaining mass (m_r) to the original mass (m_o) of the fuel for both the configurations of the wood cribs: Case 1 (low porosity) and Case 2 (high porosity).

generation is also affected by the fuel surface area. However, due to the limitation of large-scale fire tests, finding representative fuel that varies in surface area and fuel porosity proved challenging. Specifically, large wooden blocks in large-scale tests might self-extinguish due to charring layers, which could inherently impact the test results, diverging from our research objectives. Therefore, for a qualitative understanding of the effect of surface area, the authors conducted a simple calorimeter test. Along with the large-scale experiment, to illustrate the variation of HRR due to differences in fuel porosity and surface area, a cone calorimeter test has been conducted. In the bench scale experiments, two cases were used. In the first case, a solid block of wood measuring $10 \times 10 \times 3$ cm^3 was used, as shown in Figure 6. In Case 2, 12 sticks, each 10 cm long with a diameter of 1 cm, were stacked to a height of 3 cm. The same wood was used for both cases and exposed to irradiation of 50 kW/m^2. The HRR was calculated based on oxygen calorimetry.[34] Figure 6A shows the significantly higher HRR for the case when fuel was placed in the form of sticks compared to the solid block. These results are intuitive and confirm the well-established analytical, numerical simulations (Section 3) and using fire dynamics principles.[19] Figure 6B shows the ratio of the remaining mass (m_r) to the original mass (m_o). As shown in Figure 6 the HRR and mass consumption rate are much higher in sticks compared with solid block. The mass-loss rate is lower for block; however, it keeps burning for a longer period (Equation 1). The current large-scale experiment, presented in Section 2, justifies the findings from the calorimetry tests of high HRR for high porosity fuel.

3 | NUMERICAL STUDY

3.1 | Critical fire scenario

To bridge the gap between experimental findings and real-world fire scenarios, CFD simulations were employed in this section to explore the influence of air gaps between the fuel and its surface area on variations in HRR and fire behaviours. Although ventilation-controlled
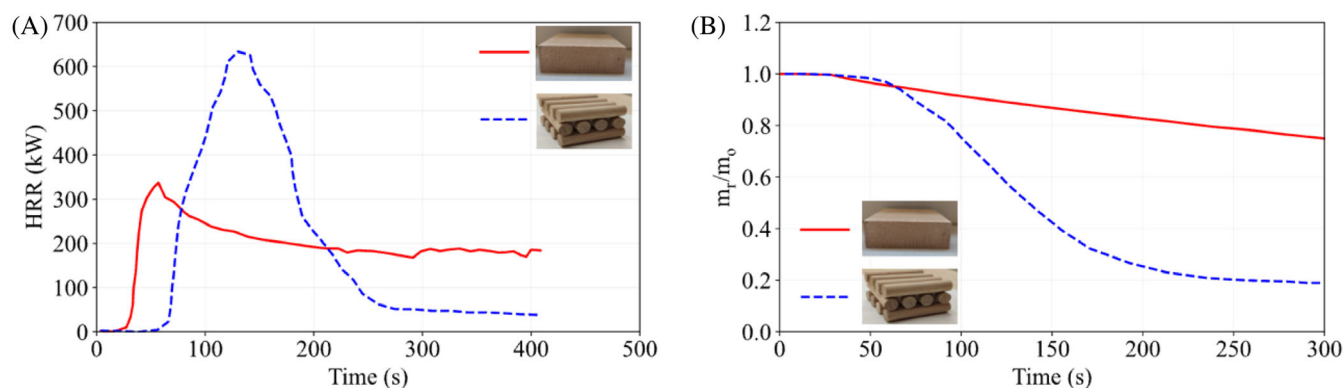
FIGURE 6 The comparisons between two cases of different fuel surface areas, that is, block and sticks: (A) HRR; and (B) ratio of the remaining mass (m_r) to the original mass (m_o).

fires are identified as critical stages in prescriptive design for traditional small compartments, their applicability to modern high-rise buildings may not always be straightforward. Observations from fire incidents reveal that due to changes in boundary conditions during a fire, such as glass breakage and failure of compartmentalization, determining the onset of ventilation-controlled fire becomes challenging. Therefore, an investigation that considers both more realistic ventilation and fuel load conditions is important to further explore fire spread and development in PBD. PBDs are based on the "goals and objectives" where the designers need to demonstrate that the proposed design achieves the desired fire safety goal. The designer presents various fire scenarios based on the objective. The minimum objectives of the PBD are to limit the fire within the fire compartment and affect the nearby buildings.[23] The above experiments show that even for the same fuel load fire behaves differently. The authors numerically demonstrate the effect of fuel distribution on the fire spread and suggest designers to include such scenarios in "fire safety designs". Since the tragic event of WTC, the use of the capabilities of the computational fluid dynamics CFD for fire simulation has increased extensively, particularly for modelling smoke movement in the fire-safety PBD. To conduct numerical study for the effect of fuel distribution and fire spread phenomenon, Fire Dynamics Simulator (FDS) 6.7—developed by National Institute of Science and Technology—is used.[35] Among the researchers and practicing engineers for fire engineering design, the FDS is the most popular CFD fire modelling software globally. It is worth mentioning here that it is still not possible to carry out an accurate computational study for the effect of porosity due to the limitation of the computational modelling of the pyrolysis process of the solid fuel. It may be required to carry out the direct numerical simulation for such study, which is generally not a practical approach for large computational domains. Therefore, the numerical study presented in these sections is for qualitative understanding and providing the methods to conduct a large-scale experiment for such cases, as presented in Section 2. The data from experimental studies can be used for calibrating the CFD models that can be further utilised for PBD.

To study the effects of the porosity (spacing between the fuel in case of numerical study) and fuel distribution, a compartment of $6 \times 6 \times 3$ m³ is generated in FDS. The size of the computational domain to carry out the fire simulations is $8 \times 8 \times 4$ m³. Two different set-ups of fuel distribution are studied. The same fuel density is considered for both configurations. It is worth noting that the fuel size is different for both cases ($1 \times 0.4 \times 0.2$ m³ and $1 \times 1 \times 0.35$ m³), therefore, there are more blocks for the smaller one, as a result, the surface area is also higher. Furthermore, two different ventilation conditions are presented to understand the effects of the openings in the compartments. In the first case, a soffit is provided on three sides of the compartment, and in another configuration, all soffits are removed, and the compartment is kept open to three sides (similar to the experimental conditions). The open compartment presents the case of a fire in a large compartment. Figure 7 shows the configuration for all four cases, that is, Case A: high porosity with soffits, Case B: high porosity without soffit (open), Case C: low porosity with soffits, and Case D: low porosity without soffit (open). Figure 7 also shows the dimensions of the block of the fuel for each configuration. The material properties of the combustibles for simulation were assigned according to SFPE Handbook.[29] The primary motive of these numerical simulations is to understand qualitatively the fire behaviour in the above-mentioned configurations. Such configurations of the fire can be used in further experimental studies. Furthermore, in business and storage occupancies, such configurations of the fuel can be found. This study shows that despite having the same fuel load density, the fire behaves differently and can be more severe than the other. After performing a few numerical tests as sensitivity analysis, the cell size of 0.1 m was chosen when the variation in gas temperatures was negligible. The chosen cell size of 0.1 m represents a reasonable fire spread at a lower computational cost. As discussed, due to the simplification used in CFD modelling for solid phase pyrolysis, to simulate the fire spread, the "surface ignition method" available in FDS was used. The ignition temperature of the fuel surface (250°C in the case of wood) was set for its ignition to simulate the fire spread.
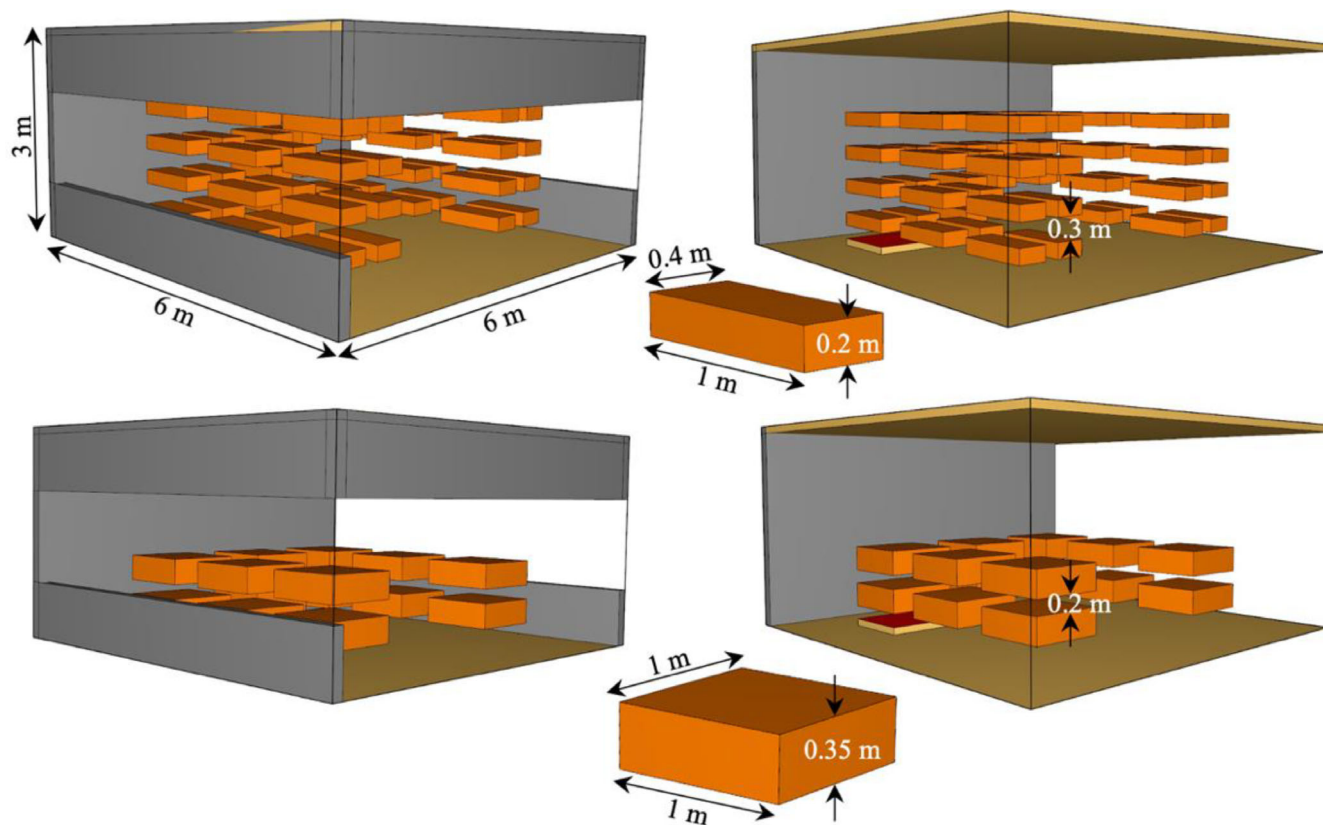
FIGURE 7 Four different cases of numerical tests: (A) Case A: high porosity with soffit; (B) Case B: high porosity without soffit; (C) Case C: low porosity with soffit; and (D) Case D: low porosity without soffit.
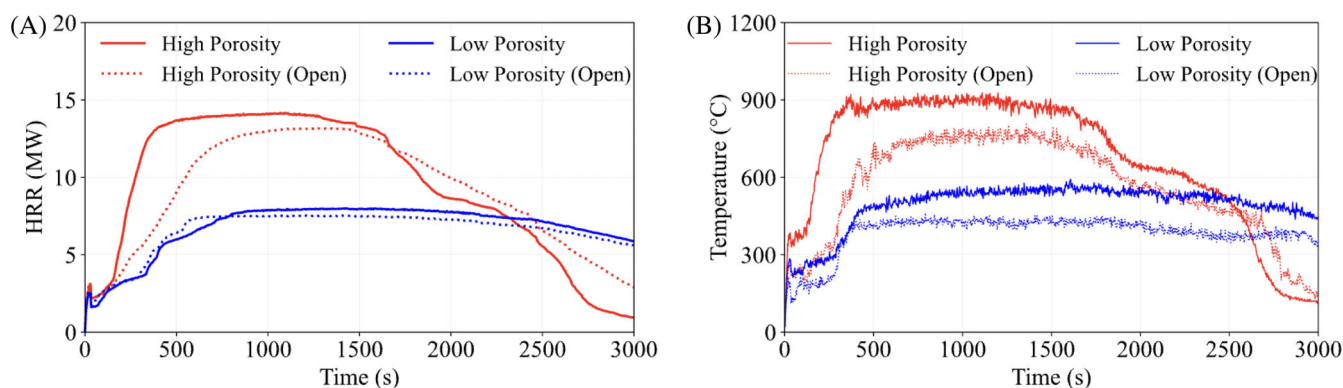

FIGURE 8 The comparisons for all four cases, that is, Case A–Case D: (A) HRR; and (B) gas temperatures.

Figure 8A shows the HRR for all cases. The HRR for high porosity (Case A and Case B) is much higher than the low porosity configurations (Case C and Case D). The peak HRR for high porosity fuel configurations reaches around 1.3–1.4 MW, however for low porosity cases, the peak HRR is between 0.7 and 0.8 MW. The high value of the HRR for the high porosity case can be explained by the high surface area of the exposed fuel. In an experimental study performed by Gross and Robertson,[36] a considerably higher burning rate was observed for fuel distribution with the higher surface area under unrestricted ventilation conditions. This behaviour validates the observations made in this study, as Cases A and B show the higher burning rate due to the availability of higher fuel surface area compared to Case C and Case D.

Besides the fuel porosity (as discussed in Section 2), surface area and fuel thickness play an important role in the burning rate (Equation 2) (the effect of surface area is also presented in the bench scale test in Section 2.2). The burning rate can also be presented using Equation 4.[29] Equation 4 shows that the burning rate ($\dot{m}$) is inversely proportional to the thickness of fuel (*D*) (0.2 and 0.35 m for Case A and Case B, respectively[29]). By conducting theoretical and
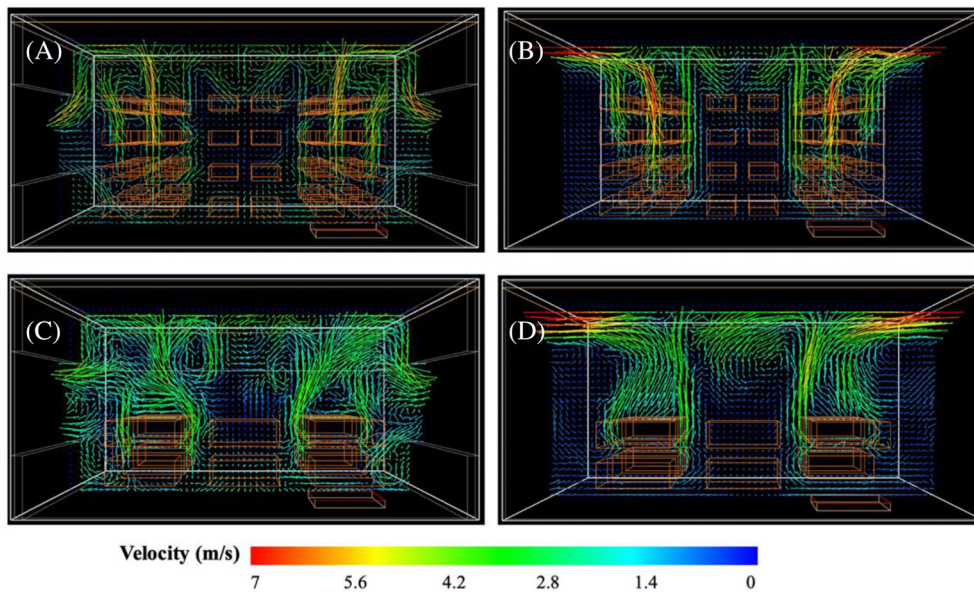
FIGURE 9 Velocity vectors after 600 s since ignition for (A) Case A; (B) Case B; (C) Case C; and (D) Case D.

experimental studies, a similar relationship between the burning rate and the thickness of the fuel bed has been presented by Block[37] (Equation 5).

$$\dot{m} = \frac{4}{D} m_o v_p \left(\frac{m}{m_o} \right)^{\frac{1}{2}} \tag{4}$$

where m_o is original mass and v_p is the regression velocity, which depends on the type of the material.[29]

$$\dot{m} = \frac{C}{D^{0.5}} \tag{5}$$

where C is the material property and is independent of the size and geometry of the fuel.

Although the HRR for soffit and non-soffit cases are quite similar in both configurations (Cases A and B and Cases C and D), the variation in the temperatures observed for different ventilation conditions is quite significant. Figure 8B shows the gas temperature–time history recorded near the ceiling. In the case of the high porosity, the maximum temperature reaches nearly 900°C. On the other hand, the maximum temperature in the low porosity is below 600°C. The variation of the maximum gas temperatures between the soffit and non-soffit conditions is around 200 and 150°C for high porosity and low porosity cases, respectively. In the case of the soffits, higher temperatures are obtained mainly because of the temperatures raised by the deep smoke layer, which is not generated in the open boundaries.[38] In a number of experiments carried out by Wakamatsu et al.[39] and Hasemi et al.[30] much higher temperatures have been obtained for soffit cases.

Not only the accumulation of smoke raised the temperatures, but also the air entrainment is one of the major causes of the temperature differences for the soffit and non-soffit cases. Figure 9 shows the contour plots for velocity profile obtained from the CFD simulations for all cases at X = 3 m (Centre of the room). During the combustion process of the fuel, the products of combustion such as hot gases and soot rise due to buoyancy and escape the compartment through the openings. It allows drawing cool air inside, as illustrated in Figure 9. Kawagoe and Sekine[40] conducted an experiment to study such phenomenon. An empirical relationship (Equation 6) between the heat losses and the mass flow rate of the cooler air entering the compartment has been presented. The colder air entering the compartment replaces the hot gases and reduces the overall temperatures. When comparing the effects of the soffit on overall temperatures inside the compartment, higher temperatures are observed in cases with the soffit. Figure 9B,D (Case B and Case D) show that the hot gases leaving the compartment have higher velocities than the compartments with soffits (Figure 9A,C) (Case A and Case C). The replacement of the hot gases with the colder air reduces the overall temperatures of the compartment.

$$Q_L = \dot{m} G_o (T_g - T_a) C_p \tag{6}$$

where G_o (m³kg⁻¹) is the volume of the combustion gases produced by the fire. T_g and T_a are the gas temperature and outside air temperature, respectively. $\dot{m}$ (kgs⁻¹) and C_p (kJm⁻³K⁻¹) are the mass flow rate of burning gases and the specific heat of the hot gases, respectively.

$$\dot{m}_{in} \propto \dot{m} \tag{7}$$

$$\dot{m}_{out} \propto \dot{m} \tag{8}$$

As presented by Magnusson and Thelandersson in their work[41] that the rate of incoming colder air ($\dot{m}_{in}$) and outgoing hot gases ($\dot{m}_{out}$) is also a function of the burning rate (Equations 7 and 8). Therefore, the volumes of the cool air coming in and hot gases going out increases with an increase in the burning rate. As the burning rate is much higher for Case A and Case B compared to Case C and Case D,

TABLE 1 Effects of soffit and porosity on the overall temperatures.

Cases	Description	Soffit effect	Porosity effect	Overall temperatures	Reasons
Case A	High porosity with soffit	Low velocities of gases	Highest burning rate	Highest	The burning rate increased temperatures.
Case B	High porosity without soffit	High velocities of gases	Nearly similar to Case A	High	High gas velocities bring in colder air faster, resulting in lower temperatures compared to Case A. However, with higher burning rates, temperatures are higher than in Case C.
Case C	Low porosity with soffit	Low velocities of gases	Low burning rate	Low	The burning rate is much lower than in Case A, resulting in lower temperatures. However, the slower replenishment of colder air makes the temperature higher than in Case D.
Case D	Low porosity without soffit	High velocities of gases	Nearly similar to Case C	Lowest	High velocities quickly replace hot gases with colder air, reducing the overall temperatures.
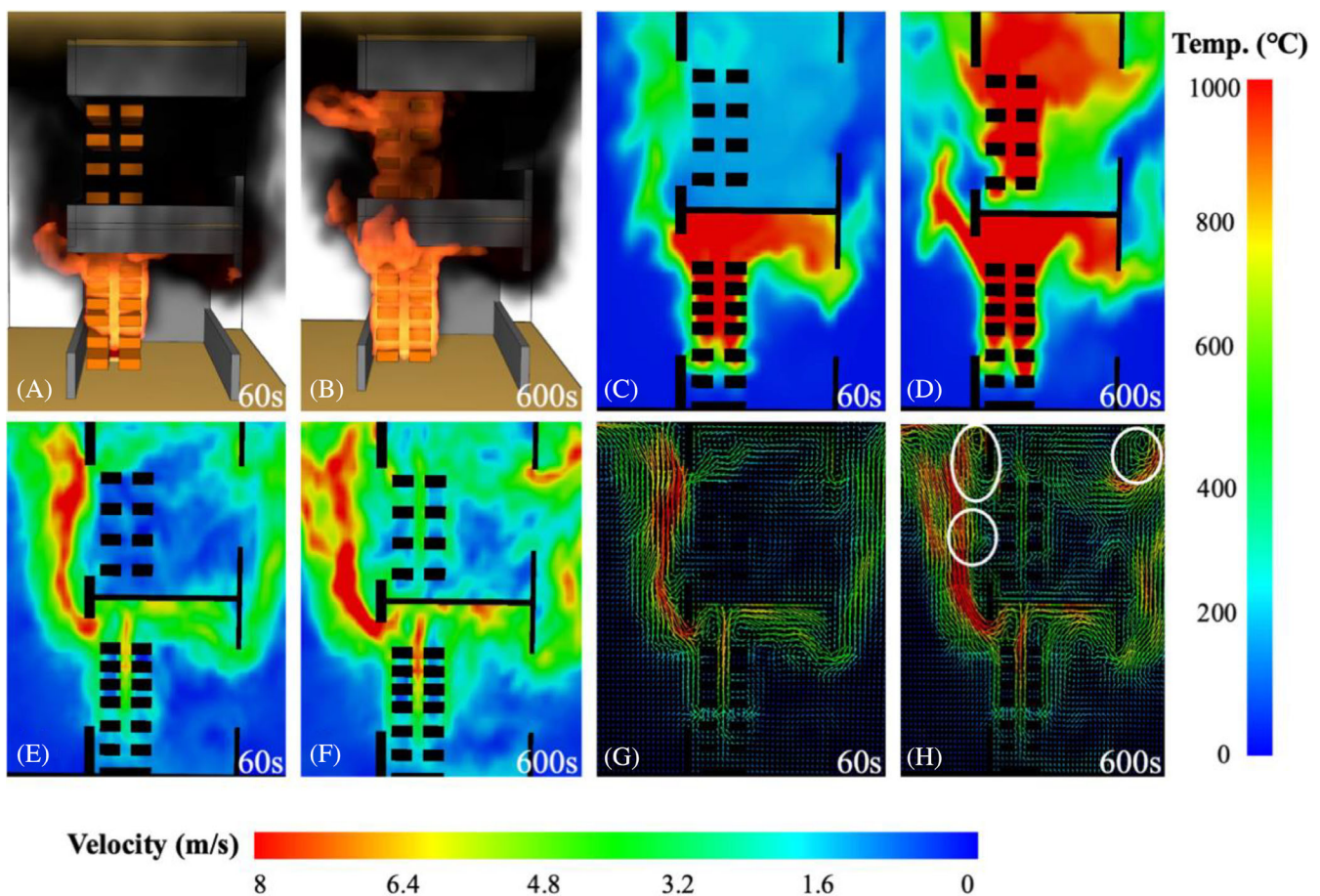
FIGURE 10 Simulation of vertical fire spread for two floor fire the vertical fire spread for high porosity cases at 60 s and 600 s: (A) and (B) fire; (C) and (D) temperature contour; (E) and (F) velocity contour; and (G) and (H) velocity vector.

more mass of hot air escapes from the compartment, and to maintain the equilibrium, an equivalent volume of cool air is drawn inside the compartment. The burning rate has a dominant effect on the overall temperature of the compartment; therefore, higher temperatures are observed in cases with high porosity. Table 1 summarizes the overall effects of porosity and soffit on compartment temperatures.

3.2 | Vertical fire spread

One of the implications of high HRR and flame height is that the fire can reach upper floors in a building. Such phenomenon has been observed in many fire accidents. The fire may reach upper floors in a high-rise building through windows, façade, or vertical openings such

as stairways and elevator shafts. In many fire accidents, the fire reached upper floors from the floor of fire origin such as MGM Grand Hotel fire (1980, USA), which took the lives of around 85 people; the Plasco Building (2017) in Tehran collapsed and claimed the lives of more than 32 people, including more than 15 firefighters.

For a qualitative understanding of the vertical spread of fire, a two-floor building (one room on each floor) model is generated in FDS. Each room of floor area $4 \times 4 \, \text{m}^2$ and 3 m high is modelled as shown in Figure 10A. The case of high porosity is evaluated to represent the vertical fire spread. As the flame height depends on the HRR, it is clear from Section 2 that the HRR for the low porosity case is much lower. Figure 10A,B shows the computational model of the two-floor geometry at 60 and 600 s since ignition. It can be seen in Figure 10 that once the fire started, it grows, and flames can be seen coming out through the openings and reaching the upper floor. Figure 10 also shows the temperature and velocity contour plots, and velocity vectors at the centre of the compartment (x = 1.5 m). Figure 10C shows that very high temperatures are observed near the openings at lower floors during the early stages of the fire, and also gases are leaving the compartment at high velocity (Figure 10E,G). It is clear from Figure 10 that due to the buoyancy and stack effect (entrainment of air due to temperature differences between two regions of a building), hot gases travel upward and reach the upper floors. The openings (sufficient ventilation) allow a high volume of fresh air to enter continuously inside the fire compartment and keep the fire in the fuel-controlled regime. The higher velocity of incoming and outgoing gases makes the rapid replacement of the hot gases with the fresh air inside the compartment; eventually, the faster burning rate of the fuel is observed.

In a numerical investigation study, Satoh and Kuwahara[42] observed that large-scale vorticities in the upward motion of the hot gases because of the entrainment of cool air. Hayeshi[43] found out that due to the oscillatory motion within the gases or flames, the flames adhere to the exterior wall and enter the upper floor through windows. Figure 10H shows the large vorticities in upward fire flows (white circles), which may have caused the fire to reach the upper floor. This oscillatory motion pushes the fire toward the wall, eventually allowing the fire to enter the upper floor. Forstrom and Sparrow[44] found that the oscillatory motion is influenced by HRR, and it gets accelerated with an increase of HRR. The HRR for the high porosity fuel is much larger than the low porosity fuel, therefore the probability of the fire reaching upper floors is higher for such cases.

It is clear from the above discussion and CFD simulations that the fuel distribution methods can greatly influence the factors that lead the fire to reach upper floors, such as oscillatory motion and flame height due to the generation of high magnitude of HRR and burning rate. Therefore, it is recommended that the impact of fuel distribution be included in fire scenarios for PBD approaches, both in deterministic and probabilistic analyses.

4 | CONCLUSIONS

The fire behaviour observed in many fire accidents clearly shows that the current fire safety design practices require improvements.

The uncertainties associated with the fire behaviour arise by varying certain parameters such as fuel load, fuel distribution, ventilation, etc. Such variations make each fire a unique fire scenario. To demonstrate the effects of the porosity between the fuel, a few experiments were performed using the two configurations of wood crib. Furthermore, the effects of the fuel distribution and smoke layer are illustrated by carrying out the CFD simulations. The key findings in the current papers are listed below:

- Even for the same fuel load, the fire behaves differently. In the high porosity case, much higher values of HRR and MLR are observed.
- Flame height and gas temperatures are also higher for the high porous wood crib configuration. It suggests that flames may reach the ceilings if the fuel is loosely distributed within a compartment.
- The slow burning rate for low porous material extends the fire duration, and the fuel was kept burning for a longer period.
- The CFD simulations show the effect of the fuel distribution, where much higher differences in temperatures and HRRs are obtained for the same fuel load density but with different surface areas.
- Vertical fire spread is presented using the CFD simulation for the high porous case. It can be deduced that factors such as buoyancy, stack effect, oscillatory motion, and most importantly the height of the fuel influence the fire to reach the upper floors.

Due to the current limitations of the computational modelling of solid fuel pyrolysis, it is required to conduct experiments of different fuel configurations. The data from the experiments can further be used for calibrating the CFD models. The CFD is widely used in PBD, and it is recommended that a designer must include effect of fuel distribution in terms of fire spread from lower floors to upper floors.

NOMENCLATURE

CFD	computational fluid dynamics
DNS	direct numerical simulation
FDS	fire dynamics simulator
fTFM	flame extension travelling fire model
HRR	heat release rate
iTFM	improved travelling fires methodology
MLR	mass loss rate
NIST	National Institute of Science and Technology
PBD	performance-based design
SFPE	society of fire protection engineering
TFM	travelling fires methodology
WTC	World Trade Centre

ORCID

Zhuojun Nan https://orcid.org/0000-0001-8189-5448

REFERENCES

1. Ahrens M. *High-Rise Building Fires*. National Fire Protection Association; 2016. doi:10.20965/jdr.2007.p0236
2. NIST. NIST NCSTAR 1: Final report on the collapse of the world trade center building 7. 2008.
3. NIST. NIST NCSTAR 1: Final report on the collapse of the world trade centre towers. 2005.
4. Khan AA, Domada RVV, Huang X, Ali Khan M, Usmani AS. Modeling the collapse of the Plasco Building part I: reconstruction of fire. Build Simul. 2021.
5. Torero JL. Grenfell Tower Inquiry: Professor Jose Torero Expert Report (Phase 1 - supplemental), JTOS0000001. 2018.
6. Prasad K, Baum HR. Coupled fire dynamics and thermal response of complex building structures. *Proc Combust Inst*. 2005;30(2):2255-2262. doi:10.1016/j.proci.2004.08.118
7. Usmani A, Chung YC, Torero J. How did the WTC towers collapse: a new theory. *Fire Saf J*. 2003;38(6):501-533.
8. Clifton C. Fire models for large firecells, HERA Report. 1996:83.
9. Stern-Gottfried J, Rein G. Travelling fires for structural design—part I: literature review. *Fire Saf J*. 2012;54:74-85. doi:10.1016/j.firesaf.2012.06.003
10. Stern-Gottfried J, Rein G. Travelling fires for structural design-part II: design methodology. *Fire Saf J*. 2012;54:96-112. doi:10.1016/j.firesaf.2012.06.011
11. Rackauskaite E, Hamel C, Law A, Rein G. Improved formulation of travelling fires and application to concrete and steel structures. *Structure*. 2015;3:250-260. doi:10.1016/j.istruc.2015.06.001
12. Heidari M, Kotsovinos P, Rein G. Flame extension and the near field under the ceiling for travelling fires inside large compartments. *Fire Mater*. 2019;44(3):423-436. doi:10.1002/fam.2773
13. Dai X, Welch S, Usmani A. A critical review of "travelling fire" scenarios for performance-based structural engineering. *Fire Saf J*. 2017; 91(May):568-578. doi:10.1016/j.firesaf.2017.04.001
14. Dai X. *An Extended Travelling Fire Method Framework with an OpenSees-Based Integrated Tool SIFBuilder*. The University of Edinburgh; 2018.
15. Dai X, Welch S, Vassart O, et al. An extended travelling fire method framework for performance-based structural design. *Fire Mater*. 2020;44(3):437-457. doi:10.1002/fam.2810
16. Nan Z, Khan AA, Zhang X, Jiang L, Huang X, Usmani A. Fire spread and burning dynamics of non-uniform wood crib for evolved design fire scenarios. *Fire Saf J*. 2023;140:103840. doi:10.1016/j.firesaf.2023.103840
17. Eurocode I. BS EN 1991-1-2:2002. Eurocode 1: actions of structures—part 1-2: General actions—actions on structures exposed to fire. 2002.
18. Chow WK, Kot HT. Hotel fires in Hong Kong. *Int J Hosp Manag*. 1989;8(4):271-281. doi:10.1016/0278-4319(89)90004-2
19. Khan MA, Khan AA, Usmani AS, Huang X. Can fire cause the collapse of Plasco Building: A numerical investigation. *Fire Mater*. 2022;46(3):560-575.
20. NFPA. NFPA 557: standard for the determination of fire loads for use in structural fire protection design. National Fire Protection Association, Quincy, MA. 2020.
21. Khan AA, Usmani AS, Torero JL. Evolution of fire models for estimating structural fire-resistance. *Fire Saf J*. 2021;124:103367.
22. Ahmadi MT, Aghakouchak AA, Mirghaderi R, et al. Collapse of the 16-story Plasco Building in Tehran due to fire. *Fire Technol*. 2020; 56(2):769-799. doi:10.1007/s10694-019-00903-y
23. ISO. ISO 23932-1:2018 fire safety engineering—general principles, Part 1: General. Internaional Organization of Standardization, Geneva, Switzerland. 2018.
24. Thomas PH, Heselden AJM. Fully developed fires in single compartments. Fire Research Note No 923, Fire Research Station, Borehamwood, UK. 1972.
25. Thomas PH, Heselden AJ, Law M. Fully-Developed Compartment Fires-Two Kinds of Behaviour. no.(28):1967.
26. Kawagoe K. Fire behaviour in rooms—Report No. 27. 1958.
27. Torero JL, Majdalani AH, Cecilia AE, Cowlard A. Revisiting the compartment fire. *Fire Saf Sci*. 2014;11:28-45. doi:10.3801/IAFSS.FSS.11-28
28. Kirby BR, Wainman DE, Tomlinson LN, Kay TR, Peacock BN. Natural fires in large scale compartments. *Int J Eng Perform-Based Fire Codes*. 1999;1(2):43-58.
29. SFPE. *SFPE Handbook of Fire Protection Engineering*. Vol 5. 5th ed. Springer; 2016. doi:10.1016/s0379-7112(97)00022-2
30. Hasemi Y, Yokobayashi Y, Wakamatsu T, Ptchelintsev AV. Modelling of heating mechanism and thermal response of structural components exposed to localised fires.Thirteenth Meeting of the UJNR Planel on Fire Research and Safety. 1996.
31. Law M. Structural engineering 1983;1:25.
32. Gross D. Experiments on the burning of cross piles of wood. *J Res Natl Bureau*. 1962;66C(2):99-105.
33. BS EN. Eurocode 1: Actions on structures. *The European Standard EN 1991-1-4*. 2005;3(1):152.
34. Quintiere J. *Fundamentals of Fire Phenomena*. John Wiley; 2006. doi:10.1002/0470091150
35. McGrattan K, Hostikka S, McDermott R, Floyd J, Weinschenk C, Overhold K. *Sixth Edition Fire Dynamics Simulator User's Guide (FDS)*. 6th ed. NIST Special Publication 1019; 2016. doi:10.6028/NIST.SP.1019
36. Gross D, Robertseon AF. Experimental Fires in Enclosures. *Tenth Symposium (International) on Combustion*. 1965;(9783319288611):931–942. doi:10.1007/978-3-319-28862-8_5
37. Block JA. A theoretical and experimental study of non-propagating free-burning fire. *Symp (Int) Combust*. 1971;13(1):971-978.
38. Khan AA, Nan Z, Jiang L, et al. Model characterisation of localised burning impact from localised fire tests to travelling fire scenarios. *J Build Eng*. 2022;54(April):104601. doi:10.1016/j.jobe.2022.104601
39. Wakamatsu T, Hasemi Y. *Heating mechanism of building components exposed to a localized fire—FDM thermal analysis of a steel beam under ceiling*. Int Assoc Fire Saf Sci; 1997:335-346.
40. Kawagoe K, Sekine T. Estimation of fire temperature-time curve in rooms. 1963.
41. Magnusson SE, Thelandersson S. Temperature—time curves of complete process of fire development. 1970.
42. Satoh K, Kuwahara K. A numerical study of window-to-window propagation in high-rise building fires. In: Cox G, Langford B, eds. *Fire Safety Science*. Routledge; 2006:355-364. doi:10.4324/9780203973493
43. Hayashi K. Experimental study of upward fire propagation from an opening of fire room (in Japanese)", Report of FRI, No.57, p. 49. 1984.
44. Forstrom RJ, Sparrow EW. Experiments of buoyant plume above a heated horizontal wire. *Int J Heat Mass Transf*. 1967;10:321.
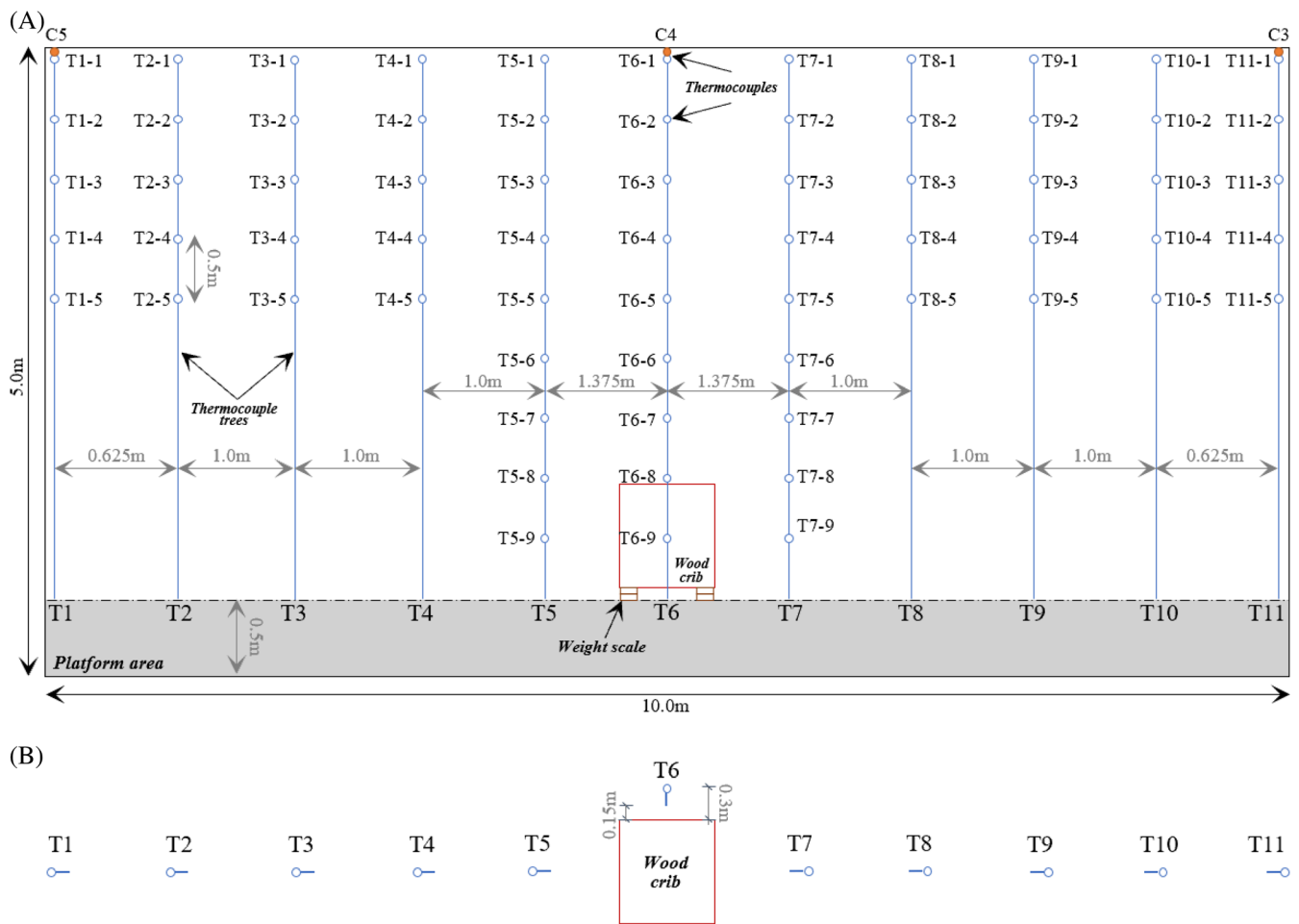
APPENDIX A

FIGURE A1 The sketch of the experimental set-up of tests with the location of sensors: (A) elevation view; and (B) plan view.